

1 **Separation of an upwelling current bounding the Juan
2 de Fuca Eddy**

3 **Jody M. Klymak^{1,2}, Susan E. Allen^{3,4}, Stephanie Waterman³**

4 ¹School of Earth and Ocean Sciences, University of Victoria, BC, Canada

5 ²Department of Physics & Astronomy, University of Victoria, BC, Canada

6 ³Department of Earth, Ocean and Atmospheric Sciences, University of British Columbia, Vancouver, BC,

7 Canada

8 ⁴Institute of Applied Mathematics, University of British Columbia, Vancouver, BC, Canada

9 **Key Points:**

- 10 • The shelf break current along Vancouver Island separates downstream of a submarine
11 bank.
- 12 • Offshore water is drawn onto the shelf and forms a sharp semi-persistent front with
13 the Juan de Fuca Eddy.
- 14 • The Eddy shows evidence of long residence times, and little evidence of deep-water
15 origin.

16 **Abstract**

17 Observations of temperature, salinity, and oxygen on the southern Vancouver Island
 18 shelf show a large-scale exchange of shelf water with offshore water, just offshore of a semi-
 19 permanent recirculation. The semi-permanent cyclonic recirculation (the Juan de Fuca
 20 Eddy) occupies a region where the shelf widens abruptly in the lee of a bank. The water
 21 in this Eddy is a mixture of offshore water and water from a buoyant coastal current. This
 22 water is well-mixed along a mixing line in temperature-salinity space, though it retains
 23 stratification, and is either rapidly mixed or has a long residence time. There is a sharp
 24 temperature-salinity front on the offshore side of this well-mixed water, no more than 1-km
 25 wide, and has no sign of instabilities. The clearest evidence of cross-front transport is found
 26 during a short tidally resolved survey over a bank, and was due to flows in the cross-bank
 27 direction driving large mixing in 50-m tall hydraulic jumps. Upstream of the recirculation
 28 there is an along-shelf current flowing equatorward. However the whole current separates
 29 from the shelf before reaching the recirculation, in the lee of a bank, and is replaced by
 30 water from offshore. The separation event was also seen in sea-surface temperatures from
 31 satellite images as a tongue of cool coastal water that is ejected offshore.

32 **Plain Language Summary**

33 The southern Vancouver Island continental shelf is biologically productive due to high
 34 nutrient input from the Strait of Juan de Fuca and Salish Sea estuarine system and sub-
 35 stantial cross-shelf transport due to the complicated topography. Here we present intensive
 36 sampling of the Juan de Fuca Eddy region. The observations show that below the surface
 37 mixed layer, the water in the Eddy is low in oxygen, and has undergone substantial vertical
 38 and lateral mixing. In contrast to previous literature we find that the low oxygen in the
 39 eddy is likely because of respiration rather than being pulled from low-oxygen water in the
 40 California Undercurrent.

41 The observations also show a remarkable flow separation of the equatorward shelf
 42 current. The current is seen to detach and is pushed offshore. Such events are readily seen
 43 in satellite imagery, but our observations indicate that the separation extends the depth of
 44 the water column on the shelf, and that this separation may be partially driven by the local
 45 bathymetry. The separation is a very strong cross-shelf exchange event, and transports
 46 substantial nutrient-rich coastal water offshore to drive productivity in the deeper ocean
 47 adjacent to the continental slope.

48 **1 Introduction**

49 Cross-shelf exchange is important to the health and productivity of continental shelf
 50 regions, allowing for offshore oxygenated water to be exchanged with nutrient-rich, but
 51 oxygen-depleted, nearshore water. Cross-shelf transport usually requires ageostrophic flow,
 52 since geostrophically balanced flow will tend to follow topographic contours, often providing
 53 a barrier to lateral exchange (Brink, 2016). Mechanisms of cross-shelf exchange include
 54 internal waves and instabilities in shelf-break fronts. However, these mechanisms can be
 55 smaller in magnitude compared to intermittent three-dimensional exchange, driven by ed-
 56 dying, often catalyzed by topographic irregularity (Barth et al., 2000).

57 Here we present detailed *in-situ* observations from the southern Vancouver Island shelf,
 58 collected in summer 2013, and sampled by a rapid profiling vehicle equipped with a CTD
 59 and oxygen sensor, supplemented by traditional hydrographic surveys bracketing the high
 60 resolution observations by a month. The shelf has complicated bathymetry (figure 1), with
 61 a relatively simple 50-km wide shelf poleward of our study site, that widens to over 75 km
 62 wide equatorward of La Perouse Bank. The South Vancouver Island Shelf is this wide shelf
 63 region, characterized by a number of banks, and finally is incised on the poleward side by the

64 Juan de Fuca canyon. Water from the Strait of Juan de Fuca flows poleward as a buoyant
 65 current that hugs the coast (Thomson et al., 1989; Hickey et al., 1991), while shelf water
 66 flows equatorward in the summer both forced by local winds and via teleconnections with
 67 the long, homogenous shelves equatorward off Washington and Oregon (Hickey et al., 1991;
 68 Thomson & Krassovski, 2015; Engida et al., 2016). Trapped between these two currents
 69 is a region of relatively homogenous water that has been termed the Juan de Fuca Eddy
 70 (Freeland & Denman, 1982; Freeland & McIntosh, 1989; Foreman et al., 2008; MacFadyen
 71 & Hickey, 2010), denoted “EDDY” below.

72 A goal of our study was to understand how the EDDY persists and how it exchanges
 73 water properties with offshore water. We focus on water deeper than 50m, below the sum-
 74 mer mixed layer, because this water is trackable with water mass properties, even though the
 75 EDDY is often studied from the point of view of the surface circulation [e.g.] macfadyen hickey 10.
 76 Past studies have found low oxygen concentrations in the EDDY, and inferred that water
 77 is upwelled from the California Undercurrent from as deep as 400 m (Freeland & Denman,
 78 1982; Dewey & Crawford, 1988). This inference was based on the assumption that oxygen
 79 is conservative, and hence water in the EDDY had to come from the oxygen minimum zone
 80 found further offshore (Mackas et al., 1987). This lead to hypotheses that perhaps the EDDY
 81 was fed by waters being drawn up a spur canyon (called the Spur Canyon) via ageostrophic
 82 transport from offshore to onshore due to low pressure in the EDDY center (Weaver & Hsieh,
 83 1987). Below, we will argue that there is no evidence of such transport and that oxygen is
 84 likely low because of local consumption due to respiration.

85 A second goal of our study was to better understand cross-shore exchange between
 86 shelf and offshore water. Cross-shore transport is supplied by Ekman layers in simple ge-
 87 ometries under wind forcing. However, in many locations there is also evidence of eddies
 88 and filaments driving wholesale separation of shelf currents into the deep ocean. Along
 89 the Vancouver Island shelf, large filaments or instabilities of the coastal current have been
 90 inferred using satellite images (Ikeda & Emery, 1984; Thomson & Gower, 1998). Direct
 91 observations of such filaments have been made further to the south off Cape Blanco (Barth
 92 et al., 2000), and off other coasts (Relvas & Barton, 2005). Net cross-shore transport of
 93 nutrients and chlorophyll have been found in hydrographic surveys off Vancouver Island
 94 (Mackas & Yelland, 1999), and associated with mesoscale features in geostrophic velocities
 95 and in satellite observations. The mechanisms driving such separations are poorly un-
 96 derstood, but hypotheses include coastal hydraulics leading to along-shore trapping of coastal
 97 waves (Dale & Barth, 2001), wind stress curl variations (Castelao & Barth, 2007), induced
 98 relative vorticity due to stretching of parcels that overshoot their initial isobaths due to a
 99 sudden change in downstream bathymetry dasaro 88, and, at this location, non-linear break-
 100 ing of large-scale meanders due to baroclinic instability between the wind-driven current
 101 and the California Undercurrent (Ikeda et al., 1984; Batteen, 1997).

102 In this paper we present observations of water masses on the Southern Vancouver Island
 103 Shelf collected in 2013 (section 2), presenting the data in a number of ways to highlight the
 104 important processes, with a focus on the offshore side of the EDDY region (section 3) where
 105 we consider the age of the EDDY, the steadiness of the front separating the EDDY and the
 106 offshore water, properties along the spur canyon that was believed to feed the EDDY, and
 107 a large offshore tongue of the shelf-break current and its intrusion into the interior. We
 108 discuss the origin of the EDDY and the implications of the separating jet (section 4).

109 2 Site and Methods

110 The study site was the southern portion of the Vancouver Island Shelf (figure 1a), a
 111 particularly complicated region due to the bathymetry and varied forcing. At the south end
 112 of the study site is the Juan de Fuca canyon, which feeds dense water into Juan de Fuca
 113 Strait. This dense water is mixed with fresh water from the Fraser River at the sills and
 114 archipelagos further inland and fluxes out the Strait again, where it turns poleward along

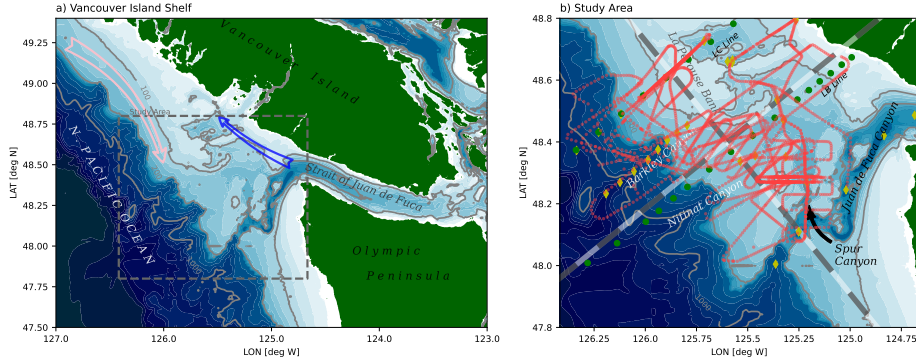


Figure 1. a) Study site on the Vancouver Island Shelf. The blue arrow indicates the direction of the Vancouver Island Coastal Current, and the pink arrow indicates southward flow of the coastal upwelling current. The dashed box indicates the approximate limits of the study area. b) The study area with hydrographic casts from the La Perouse cruises along the LB and LC Lines (green dots), hydrographic casts during the Falkor cruise (yellow diamonds), and finescale Moving Vessel Profiler casts (red dots). The coordinate system used for this paper is shown with alternating grey and white bands at 10-km intervals in the along- and cross-shore directions.

Vancouver Island to form the Vancouver Island Coastal Current. The Juan de Fuca Canyon has a notable spur canyon (Spur Canyon), that incises the shelf towards the north into the study site (figure 1b). The rest of the shelf is punctuated by a series of banks and shallow basins. La Perouse bank separates the outer shelf from a deeper inner basin and forms the poleward boundary off where the shelf widens abruptly south of 48.5 N. Equatorward, the shelf widens further, and the shelf break has a series of submarine canyons, in particular Nitnat Canyon and Barkley Canyon.

We present observations from La Perouse hydrographic surveys along the LB and LC lines, collected aboard the *CCGS Tully* from 2013-05-30 to 2013-05-31 (“May”), and 2013-09-07 to 2013-09-09 (“September”). These lines span the 50 m isobath to deep offshore, with casts every 7.5 km across shelf. The data comes from a lowered Seabird 9-11 CTD, with an SBE 43 oxygen sensor. Oxygen data have been corrected against bottle casts, and the CTD corrected for sensor offsets and thermal lags.

We focus on finescale surveys carried out between these hydrographic surveys, from 2013-08-21 to 2013-08-30. Data were collected from the *R/V Falkor* with an AML Oceanographic Moving Vessel Profiler (MVP). Data was collected analogously to data collected during similar field campaigns (Klymak et al., 2015, 2016; D’Asaro et al., 2018). The MVP was equipped with an AML Oceanographic CTD, and a Rinko Oxygen sensor with a 7-s response time foil. The MVP profiled to depths of 200 m or to within 5 m of the seafloor, whichever was shallower, and dropped at a speed of approximately 3 m s^{-1} . Data collection took place while the ship cruised at speeds between 5 and 8 kts, usually at around 6 kts, to enable fine horizontal spacing of the casts, with typical spacing of 800 m in deep water, and less in water shallower than 200 m. Data is reported for the downcast, which mostly follows a vertical path. The rapid speed of the profiling makes the oxygen measurements somewhat coarse, and probably biased due to the phase lag of the sensor, so we treat these qualitatively in this paper.

Unfortunately, neither vessel had an operational acoustic Doppler profiler during the cruises with which to make water velocity measurements.

143 Winds during the cruises were typical for the west coast of Vancouver Island, with
 144 equatorward upwelling-favorable winds during July and early August (figure 2). During
 145 the finescale survey, and for the week previous, the winds were intermittently downwelling
 146 favorable. Note that this locale is strongly affected by coastally trapped waves from further
 147 south, so doming of near-bottom isopycnals often persists despite local wind forcing, and
 148 takes a finite amount of time to spin down (Thomson & Krassovski, 2015; Engida et al.,
 149 2016).

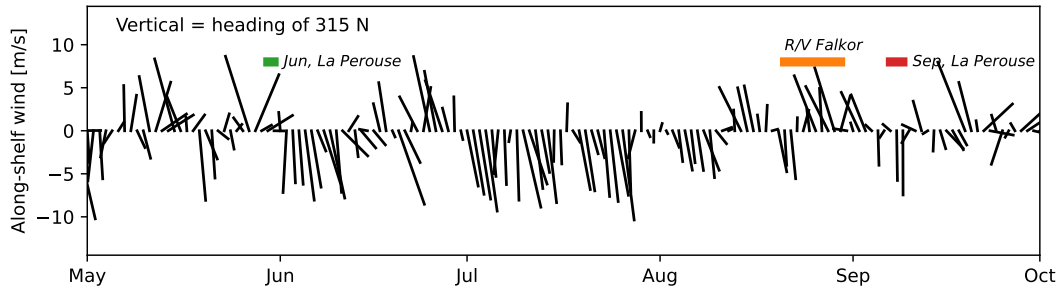


Figure 2. Wind from the La Perouse buoy (DFO, 2022). The vertical direction is along-shelf (chosen as a heading of 315 N), so vectors pointing straight down represent upwelling winds. The wind components have been low-pass filtered to one-day averages. The timing of the surveys discussed in the paper are shown as colored bands.

150

3 Observations

151

3.1 Early and late summer hydrographic surveys

152 153 154 155 156 157 158

Hydrographic sections along the LB and LC hydrographic lines highlight summer conditions on the Southern Vancouver Island Shelf and indicate some of the features we are focusing on in this paper (Figure 3). During both surveys, and along both lines, there is clear evidence of upwelling, with the 26.4 kg m^{-3} isopycnal reaching from 130 m depth offshore to shallower than 85 m over the shelf. This upwelled water tends to be low in oxygen and cool. Further onshore, the Vancouver Island Coastal Current hugs the coast, where isopycnals tilt down towards the shore, and water is warmer than offshore.

159 160 161 162

The Juan de Fuca Eddy region is observed along the LB Line (figure 3, bottom three rows), mostly inshore of 0 km. This water is cooler and lower in oxygen than along the same isopycnal further offshore. Near the surface, the isopycnals are domed, and the low-oxygen anomaly extends as high as the thin surface mixed layer.

163 164 165 166 167 168 169 170

The water upstream of the EDDY region, along the LC line, is less mixed than the EDDY water (figure 3, top three rows). It does not show as much drawdown of oxygen, and is warmer, at least offshore of La Perouse bank ($X \approx 5 \text{ km}$). Based on these properties, offshore water does not appear to make it over La Perouse bank into the onshore basin, or if it does, it does so intermittently and with substantial mixing. Note that the water along the 26.4 kg m^{-3} isopycnal becomes cooler and lower in oxygen where it intersects the shelf, consistent with both enhanced mixing near the shelf and with drawdown of oxygen by respiration.

171 172 173

The contrast in onshore and offshore waters can be clearly traced in temperature-salinity ($\theta-S$) anomalies along isopycnals (figure 4a). Denser than 26.6 kg m^{-3} , the deep water masses found offshore are largely homogenous. In the lighter water masses, there are

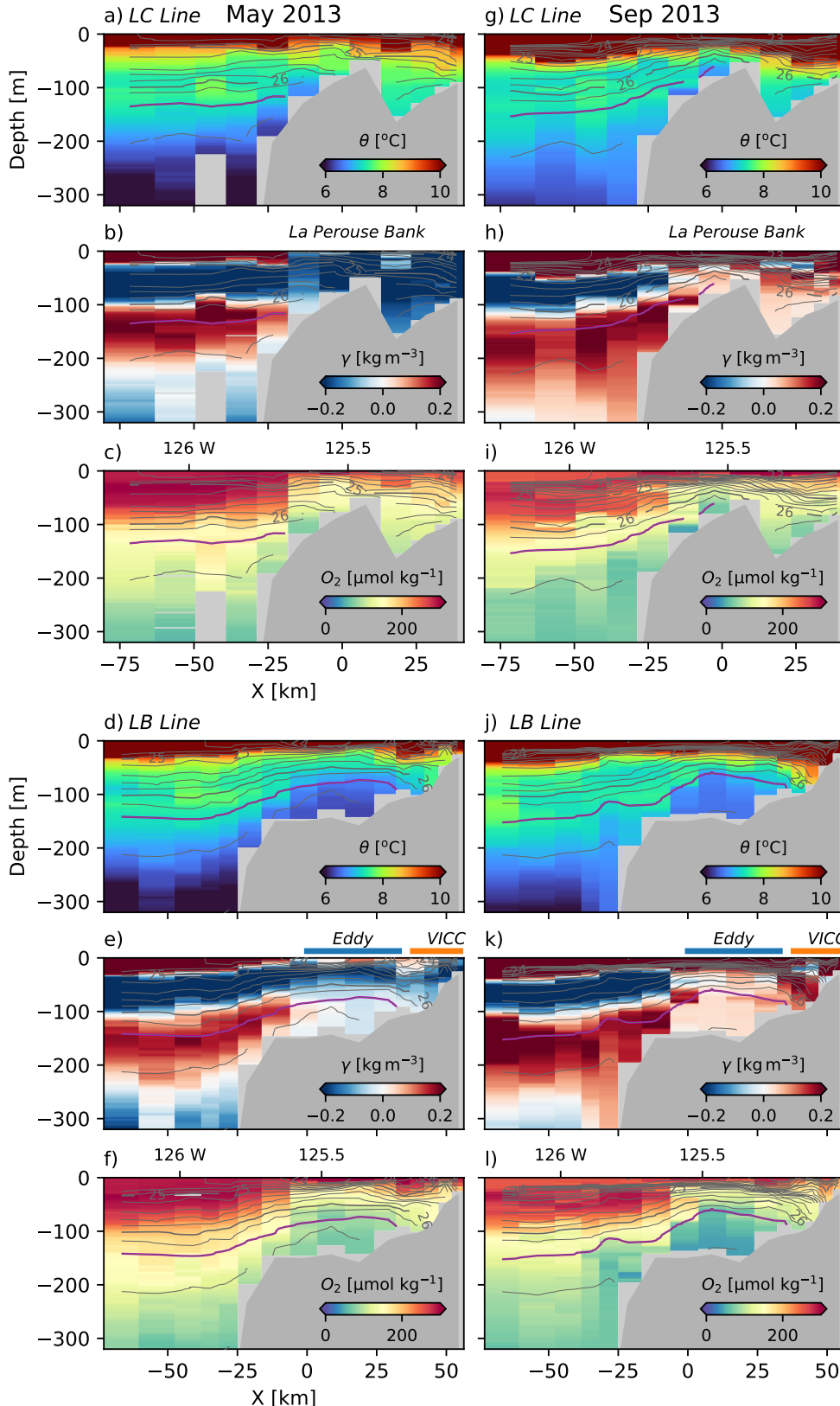


Figure 3. Observations along LC Line in May (a–c) and Sep (g–i) and LB lines in May (d–f) and Sep (j–l). X is across-shelf distance in the coordinate system shown in figure 1. Potential density is contoured every 0.2 kg m^{-3} , with the 26.4 kg m^{-3} colored magenta. Potential temperature, θ , spice anomaly, γ and oxygen concentration, O_2 , are colored for each section.

174 distinct differences between warm and salty offshore water compared to water on the shelf
175 at the same densities.

176 We use a spice anomaly defined as relative to a straight line in θ - S space (figure 4)
177 representing an approximate mixing line for water in the EDDY, and passing through the
178 points 7.75 °C, 30 psu and 6.6 °C, 35 psu. Spice anomaly for a given water sample at
179 density σ_θ is given by $\gamma = \alpha(T - T_0(\sigma_\theta)) + \beta(S - S_0(\sigma_\theta))$ where $T_0(\sigma_\theta)$, where $S_0(\sigma_\theta)$ are
180 the temperature and salinity along the mixing line at the same density as the water sample.
181 The sign convention is that a positive anomaly is warmer and saltier than data along the
182 mixing line.

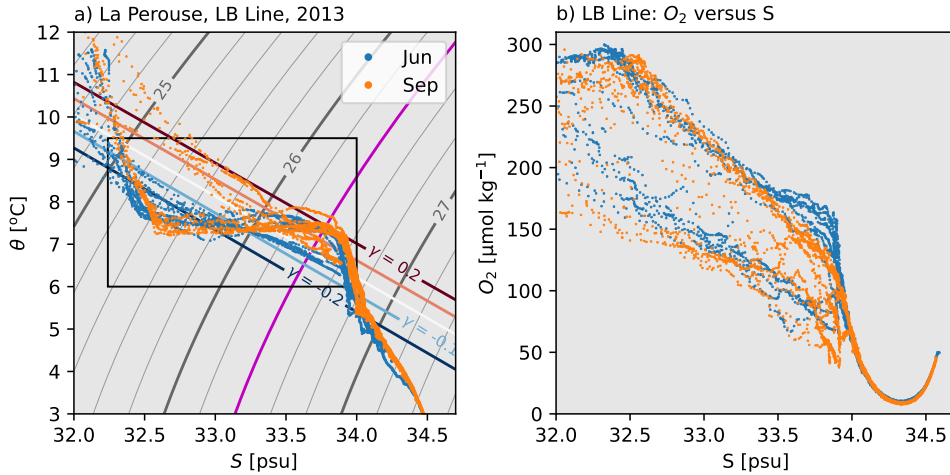


Figure 4. a) Potential temperature, θ , versus salinity, S , for the La Perouse data shown in figure 3; potential density is contoured every 0.2 kg m^{-3} , with the 26.4 kg m^{-3} colored magenta. A definition of spice anomaly is shown in this plot, and discussed in the text. The rectangle is the θ – S range used in figure 5 below. b) The same data with oxygen concentration versus salinity.

183 Using this metric of spice anomaly, offshore water tends to have high absolute values
184 (figure 3, middle rows), with a positive-anomaly layer (red) centered at 26.4 kg m^{-3} sand-
185 wiched between negative-anomaly layers above and below. On the shelf ($-10 \text{ km} < X <$
186 30 km), the distinct θ - S masses are attenuated and much closer to the defined mixing line
187 than the offshore water (closer to white in color in figure 3).

188 There are temporal changes over the summer. Away from the surface, water has
189 upwelled from deeper depths by September, but the offshore water maintains the same water
190 mass characteristics through the summer. Hugging the coast ($X > 30 \text{ km}$), the Vancouver
191 Island Coastal Current warms during the summer, and the spice anomaly goes from negative
192 to positive. In the EDDY, the water stays near the mixing line, but is cooler in the spring
193 (figure 3, LB Line, left-hand column: slightly negative spice anomaly) and warms during
194 the summer (figure 3, LB Line, right-hand column: slightly positive spice anomaly).

195 Oxygen concentration in both surveys has a similar dichotomy between the EDDY and
196 off-shelf water. Water found in the EDDY has oxygen concentrations $100 \mu\text{mol kg}^{-1}$ lower on
197 the shelf than off-shelf (figure 3, figure 4b). The very deepest water ($S \approx 33.9 \text{ psu}$) on the
198 shelf shows a further $50 \mu\text{mol kg}^{-1}$ decrease in concentration between May and September
199 along the LB line.

200 **3.2 Finescale surveys**

201 **3.2.1 Overview**

202 The finescale surveys covered most of the EDDY region, with an emphasis on the
 203 offshore edge near the shelfbreak front (figure 1). For water denser than 26 kg m^{-3} , there
 204 are three distinct water masses sampled on the shelf (figure 5). The first is offshore water,
 205 which tends to be warmer, and hence has a positive spice anomaly ($\gamma \approx 0.2 \text{ kg m}^{-3}$ along
 206 $\sigma_\theta = 26.4 \text{ kg m}^{-3}$). The second is water in the EDDY, which during this survey was found
 207 along the straight mixing line in $\theta - S$ space (figure 5, $\gamma \approx 0 \text{ kg m}^{-3}$ along $\sigma_\theta = 26.4 \text{ kg m}^{-3}$).
 208 Between these two water masses, there is a less populous mass (figure 5, $\gamma \approx 0.1 \text{ kg m}^{-3}$
 209 along $\sigma_\theta = 26.4 \text{ kg m}^{-3}$) that we demonstrate below is found on the shelf poleward of the
 210 EDDY.

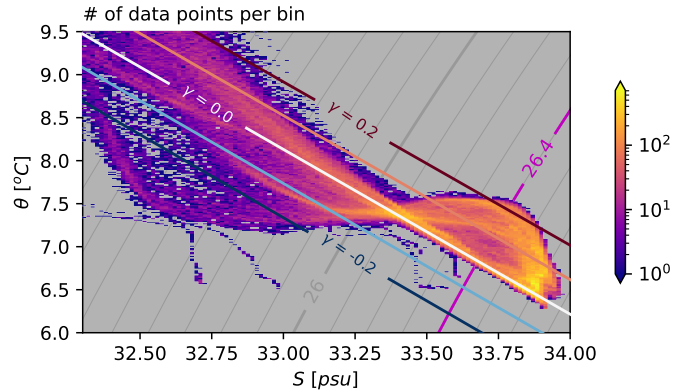


Figure 5. Binned sample density of salinity and potential temperature from the cruise, with a logarithmic color scale. Grey contours are potential density relative to the surface at intervals of 0.1 kg m^{-3} ; the magenta contour is the 26.4 kg m^{-3} isopycnal. Colored contours are spice anomaly, γ , relative to the white line labeled $\gamma = 0.0$.

211 In synthetic cross sections of spice anomaly, the EDDY is clearly identifiable as having
 212 low spice anomaly ($\gamma \approx 0 \text{ kg m}^{-3}$, figure 6c, d). This signature of well-mixed water extends
 213 from the seafloor to approximately 30 m depth, onshore of $X \approx 0 \text{ km}$. Despite lying along
 214 a mixing line, the EDDY water is still stratified. The high-spice water ($\gamma \approx 0.2 \text{ kg m}^{-3}$)
 215 is found offshore of the EDDY water, on the other side of a sharp $\theta - S$ compensated
 216 front. This front is even sharper in individual sections than in these composite sections (see
 217 section 3.2.3).

218 In contrast, the third population of partially mixed water between the EDDY and
 219 offshore water (figure 5) is all found poleward of the EDDY region (figure 6a, b) as water
 220 with a weaker spice anomaly ($\gamma \approx 0.1 \text{ kg m}^{-3}$, pink colors). This water is not as warm as
 221 offshore water, indicating some mixing with offshore water has taken place. Of note is that
 222 this intermediate water mass appears completely absent in the sections further equatorward
 223 (figure 6c, d), indicating that it is either mixed away or that it is advected elsewhere; we
 224 argue below that it is advected offshore in a large-scale tongue.

225 Oxygen saturation sections show that the deep water in the EDDY has very low oxygen
 226 saturation (figure 7c, d) compared to surrounding water (though again, we caution against
 227 the quality of these saturation values from such a fast profiling instrument with a slow
 228 response time). More oxygenated water is found offshore, and the oxygen deficit is not as
 229 strong in the poleward sections (figure 7a, b). The T/S compensated front also shows an

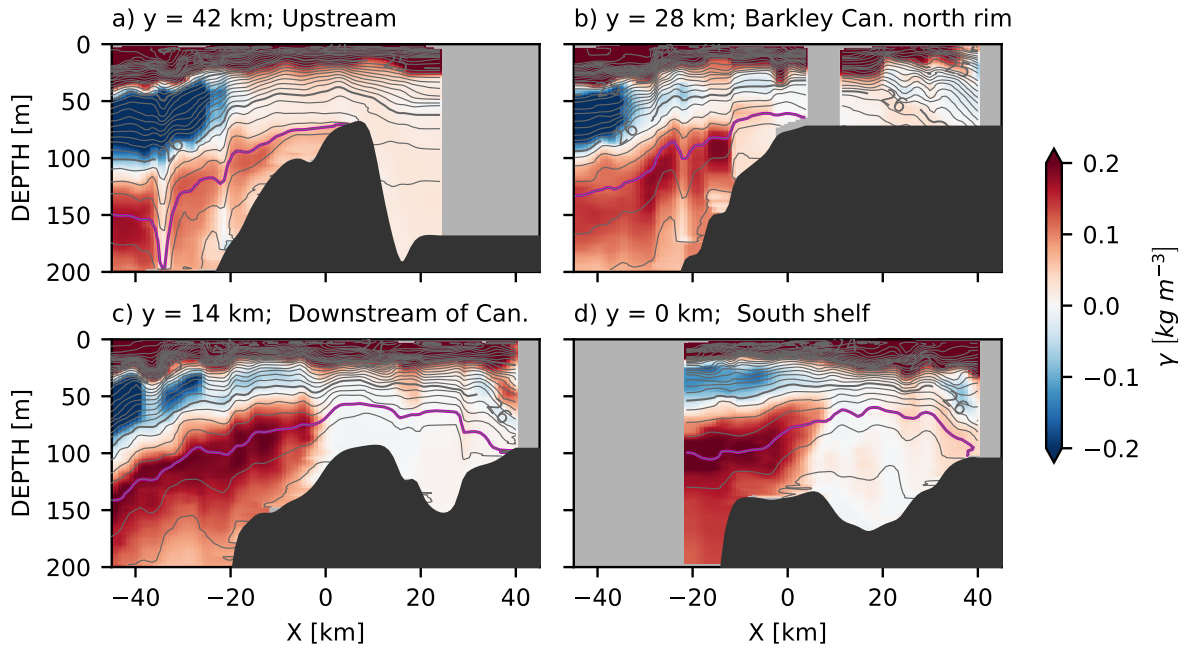


Figure 6. Synthetic sections of spice anomaly from the MVP data, projected along four lines from poleward (upstream of coastal current) a) to equatorward (downstream); the lines are shown in figure 1b). Isopycnals are contoured every $\sigma_\theta = 0.2 \text{ kg m}^{-3}$, with the $\sigma_\theta = 26.4 \text{ kg m}^{-3}$ isopycnal highlighted in magenta. Colors are spice anomaly as defined in figure 5. "BC" in panel (c) refers to Barkley Canyon.

230 abrupt transition from the EDDY water and the offshore. Note the excellent correlation
 231 between oxygen saturation and spice anomaly in figure 6.

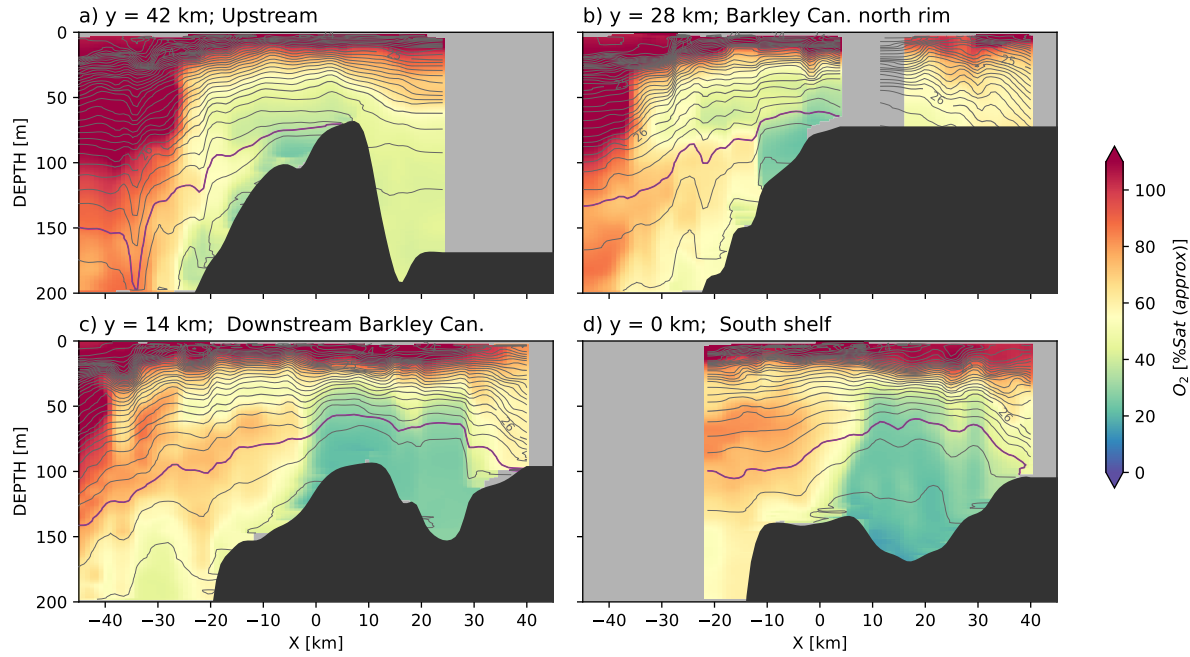


Figure 7. As in figure 6, for oxygen approximate saturation.

232 The spatial patterns are very clear when considering a map view of properties along
 233 the $\sigma_\theta = 26.4 \text{ kg m}^{-3}$ isopycnal (figure 8). There is a region onshore of the south tip of La
 234 Perouse Bank (approximately $44.5^\circ\text{N}, 125.75^\circ\text{W}$), that consists of water that is found along
 235 the mixing line (spice anomaly $\gamma \approx 0 \text{ kg m}^{-3}$) that also has low oxygen saturation. Offshore
 236 of this region is water that is very warm and salty in comparison ($\gamma > 0.15 \text{ kg m}^{-3}$), and
 237 relatively high in oxygen (saturation of approximately 60%). The region between these two
 238 water masses is very abrupt, and stretches from La Perouse Bank to a shallow bank just
 239 above the Juan de Fuca canyon (48.3°N and 125.4°W).

240 Poleward of La Perouse bank and Barkley Canyon, the water along the shelf has the
 241 weaker spice anomaly characteristic of the third water mass ($\gamma \approx 0.1 \text{ kg m}^{-3}$, light pink
 242 colors). This water is also somewhat lower in oxygen than water from offshore, though
 243 not as depleted as the water in the EDDY. This water appears to be pushed offshore just
 244 upstream of Barkley Canyon and replaced on the shelf by the warmer (high spice) offshore
 245 water.

246 3.2.2 Spur Canyon

247 The Spur Canyon leading from the Strait of Juan de Fuca has been implicated in
 248 allowing dense water to be upwelled into the EDDY. The sea surface is low in the middle
 249 of the EDDY, so it has been hypothesized that water moves up the Spur Canyon due to
 250 ageostrophic motion (Weaver & Hsieh, 1987; Freeland & Denman, 1982). This is difficult
 251 to infer from the observations collected here. Three transects up the canyon indicate that
 252 deep isopycnals slope up into the canyon (figure 9, to approximately 30 km). Continuing
 253 across the EDDY, isopycnals are largely flat until they intersect the Vancouver Island Coastal
 254 Current (80 km). The deeper isopycnals are not found in the deeper basin northeast of La
 255 Perouse bank (70 km), thus the bank is a natural poleward boundary of the EDDY.

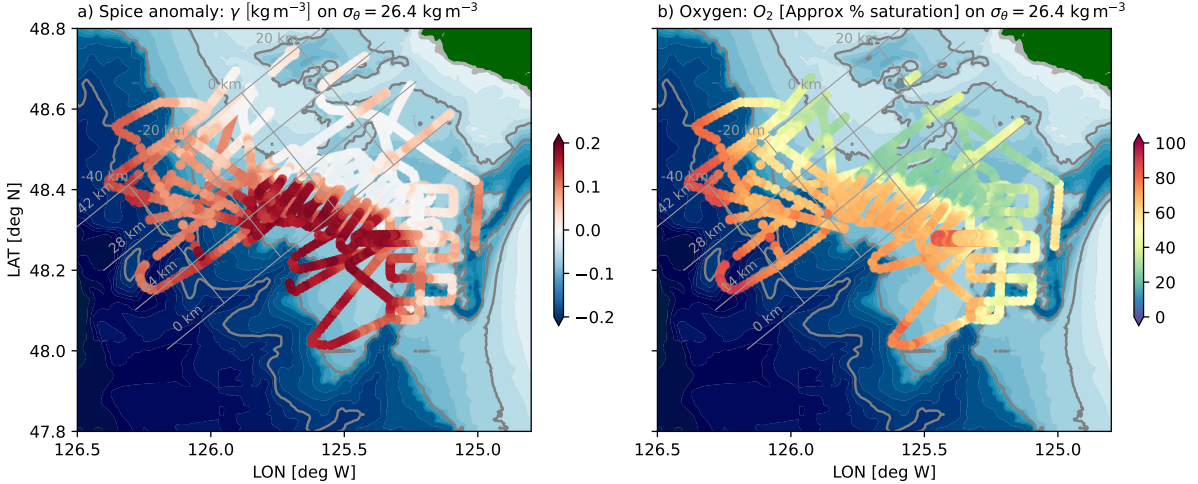


Figure 8. Spatial overview of a) the spice anomaly, and b) oxygen saturation on the $\sigma_\theta = 26.4$ kg m⁻³ isopycnal. Grey cross-slope lines are cross sections indicated in figure 6. Along-slope grey lines are every 20 km in the cross-slope direction, with $X = 0$ km near the 100-m isobath at the north end of the observation area.

Spice anomaly along the canyon indicates a transition from offshore water to EDDY water. Oxygen saturation behaves in a similar manner, though some of the incoming water has slightly lower oxygen than water inside the EDDY (not shown). Based on these sections, it is difficult to infer water motion up the canyon.

Much of the modified water in the Spur Canyon appears to come from the shelf to the west, but heavily modified by tidal mixing. A repeat tidal survey over the bank on the west side of the canyon shows a strong hydraulic response during onshore flow (17:58–21:00, figure 10). Dense water passes from the offshore side into the canyon, and plunges down the side wall before rebounding downstream. Note that the tide here is largely diurnal, so this onslope flow only occurs once a day. Given the stratification of $N \approx 6 \times 10^{-3}$ rad s⁻¹ and an overturning scale of 50 m, we might expect dissipation rates reaching $\epsilon \sim L^2 N^3 \approx 5 \times 10^{-4}$ m² s⁻³, which is three orders of magnitude higher than dissipation observed on the shelf west of this location by Dewey and Crawford (1988). This estimate of turbulence dissipation rate implies a diapycnal diffusivity of $\kappa = \gamma \epsilon / N^2 \approx 1$ m² s⁻¹, assuming a mixing efficiency of $\gamma = 0.2$. Water spills over from the offshore front into the canyon during the onshore tide. This water is rapidly mixed with surrounding water such that its strong offshore spice values are attenuated.

The turbulence found on the canyon rim makes it ambiguous if there is water moving up the canyon or not. There is a general tendency along the canyon for higher spice water to be found offshore (figure 9) but it seems likely that the source of the higher spice water is from over the bank rather than water being advected up the canyon. This tidally driven flow over the bank is the most significant source of high-spice offshore water into the eddy region identified during our surveys.

3.2.3 Frontal survey

A systematic survey through the front between the offshore water and the EDDY water demonstrates the sharpness and persistence of this front (figure 11), suggesting that it has limited exchange with the offshore region.

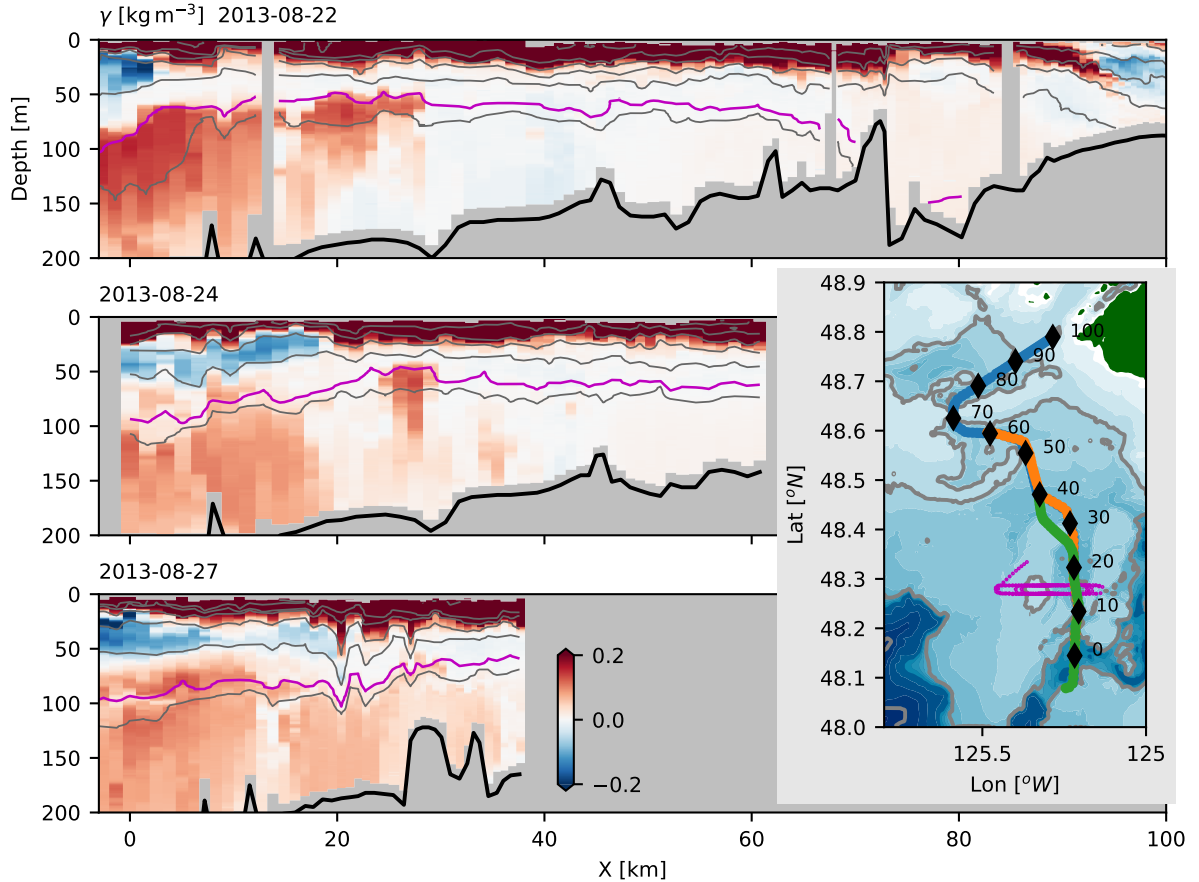


Figure 9. Spice anomaly surveys up the Spur Canyon, where X is along-canyon as defined in the map. Grey isopycnals are contoured every 0.5 kg m^{-3} , and the 26.4 kg m^{-3} isopycnal is shown in magenta. The seafloor is indicated with the thick black line. Map (lower right) shows the path taken during each survey in chronological order (blue, orange, and green). Magenta line is path taken during a cross-canyon survey (figure 10).

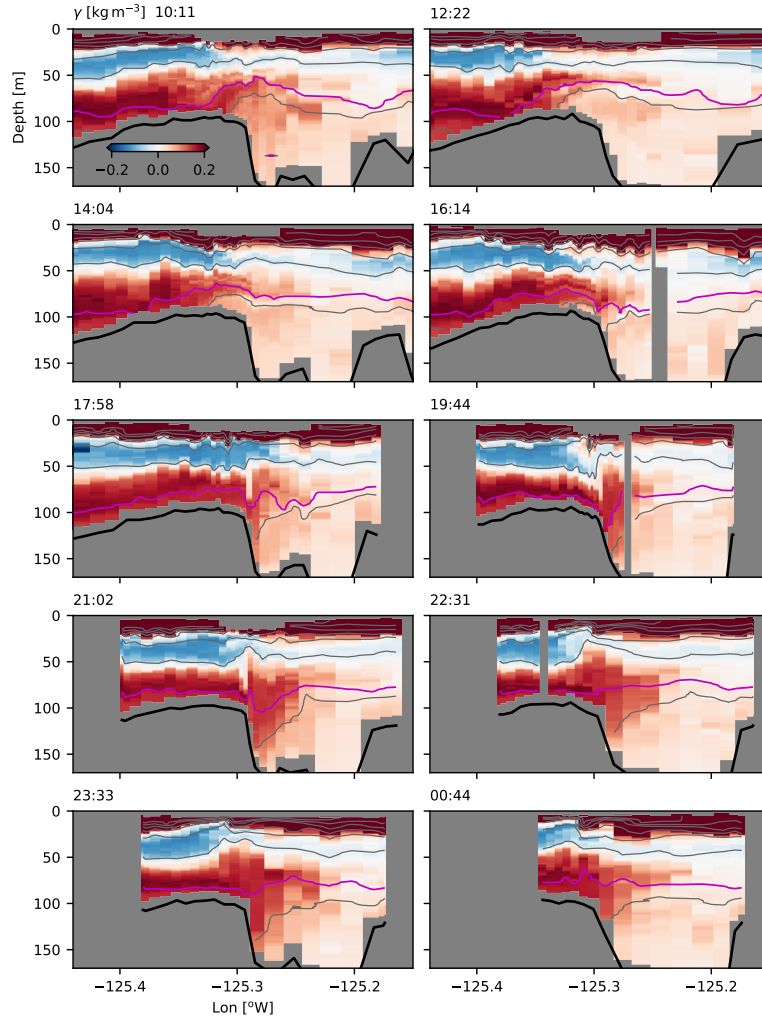


Figure 10. Spice anomaly observed in repeated, tide-resolving survey across the Spur Canyon, time is indicated in the upper left of each plot (29 August, 2013). Location of survey shown in figure 9 as a magenta line.

283 The survey started close to shore, and passed through the Vancouver Island Coastal
 284 Current (along-track 0-10 km). The coastal current forms a buoyant front, and is fresher
 285 and colder than water at the same density. This front is relatively thick, greater than 20
 286 km wide, and has partially mixed water from the surface to the foot of the front ($\gamma \approx 0.1$).

287 Offshore of this coastal current, measurements were collected crossing the front be-
 288 tween the offshore water and the EDDY water 10 times, showing its evolution following the
 289 along-shore equatorward flow. First, as noted in the composite sections, isopycnals slope up
 290 from offshore onto the shelf. In the first crossing, the front is very sharp, (along-track dis-
 291 tance 50 km) though two small tendrils can be seen separating from the front on the inshore
 292 side. Similar tendrils are found on the second crossing, perhaps a bit more separated from
 293 the front (≈ 80 km), and on the third crossing (≈ 95 km). These tendrils are made of up
 294 partially mixed water. The subsequent passes have more of this partially mixed water, such
 295 that the partially mixed front is up to 5-km wide by the fifth pass (≈ 150 km). However,
 296 the deeper isopycnals retain a sharp front, and indeed the front appears sharp again by the
 297 seventh pass at all depths (≈ 200 km).

298 There is evidence of some warmer water swirling into Eddy, particularly along isopy-
 299 cnals deeper than 26.4 kg m^{-3} . Regions of warmer (and more oxygenated) water are found
 300 in tendrils at these depths (e.g. ≈ 170 km and ≈ 185 km). The overall effect is similar to
 301 what was seen in the Gulf Stream with similar observations (Klymak et al., 2016); there
 302 are two quite distinct water masses, the Eddy water and the offshore water, as seen in the
 303 θ - S plot (figure 11c) with only a small population of samples between these two. This
 304 distribution of θ - S properties is indicative of substantial isopycnal and vertical mixing, but
 305 even these populations are relatively cut off from the main water masses, indicating that
 306 they are well-mixed on their own, in short episodic events. Regardless, this front is very
 307 sharp given that it has no density signature, indicating that there is not strong advection
 308 from offshore into the EDDY region.

309 3.3 Separation of coastal water

310 Upstream of the the sharp front between the low-spice EDDY and the high-spice off-
 311 shore water is a substantial mass of intermediate-spice water along the shelf (compare figure
 312 6a and c). This intermediate spice water is moving equatorward along the shelf upstream
 313 of the EDDY, but is pushed offshore just upstream of Barkley Canyon (figure 12). There is
 314 a tongue of intermediate-spice water (γ is pink along 26.4 kg m^{-3}) that separates from the
 315 shelf just west of 126°W . The surveys do not cross the full extent of the tongue, but it is
 316 at least 30 km wide. It also appears to end at approximately 48.2°N . This intermediate-
 317 spice water reaches from relatively shallow isopycnals to at least 26.6 kg m^{-3} (figure 12, left
 318 panel). Unfortunately, we cannot track the fate of this water mass because isopycnals tilt
 319 down offshore, below the depth limit of the MVP. The 25.5 kg m^{-3} isopycnal appears to have
 320 the tongue closer to the shelf than at 26.4 kg m^{-3} , indicating strong three-dimensionality to
 321 this feature.

322 This separating tongue is embedded in the larger scale isopycnal tilt caused by the
 323 upwelling (figure 12, right panels), so it is difficult to see dynamically what is driving this
 324 offshore push. One possibility is that it is simple flow separation caused by the water not
 325 being able to make the sharp turn around La Perouse Bank. Whatever causes it, downstream
 326 of the separation, the water is replaced by offshore water with much higher spice values.

327 There is a clear surface expression of the separating tongue in satellite imagery (fig-
 328 ure 13). Water flowing equatorward along the shelf tends to be cooler than offshore water,
 329 likely due to mixing with the colder coming out of the Strait of Juan de Fuca. On August
 330 25, there is a cold tongue of water separating from La Perouse bank, crossing isobaths and
 331 pointing south at 125.8°W . There is a cooler tendril streaming west at 48°N off the south end
 332 of this tongue. This feature is not as well-developed in the previous image (Aug. 21) perhaps
 333 indicating that it is an evolving feature. By 31 August, there is no surface expression of

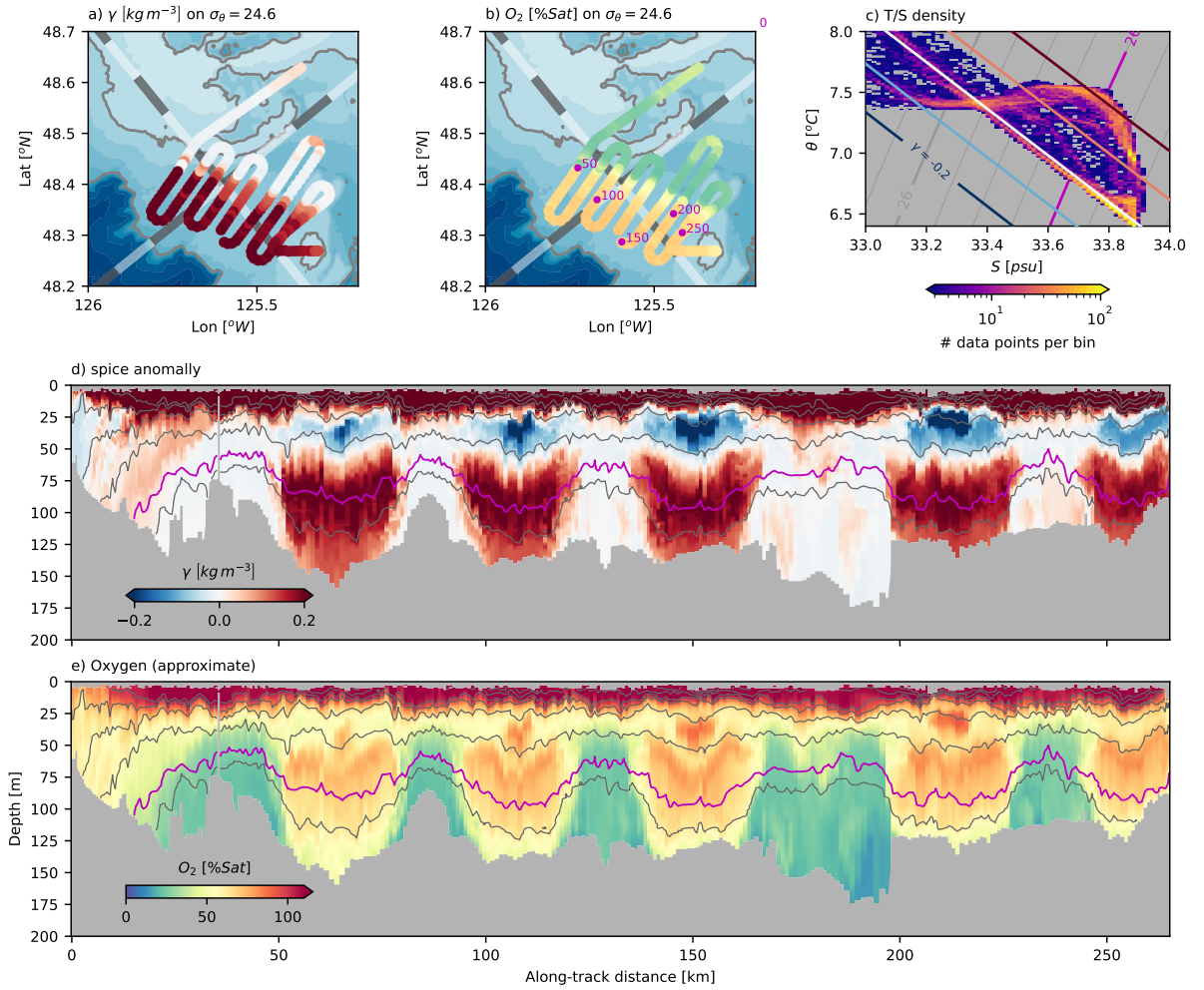


Figure 11. Data from the frontal survey a) spice anomaly along 26.4 kg m^{-3} . Grey-white alternating lines are the coordinate system, with 10-km alternating shades. b) oxygen saturation along 26.4 kg m^{-3} ; magenta dots correspond to distance along-track. c) density of data points (logscale) in this section of data. d) cross-section of spice anomaly along track. Grey isopycnals are contoured every 0.5 kg m^{-3} , and the 26.4 kg m^{-3} isopycnal is shown in magenta. e) cross-section of oxygen saturation.

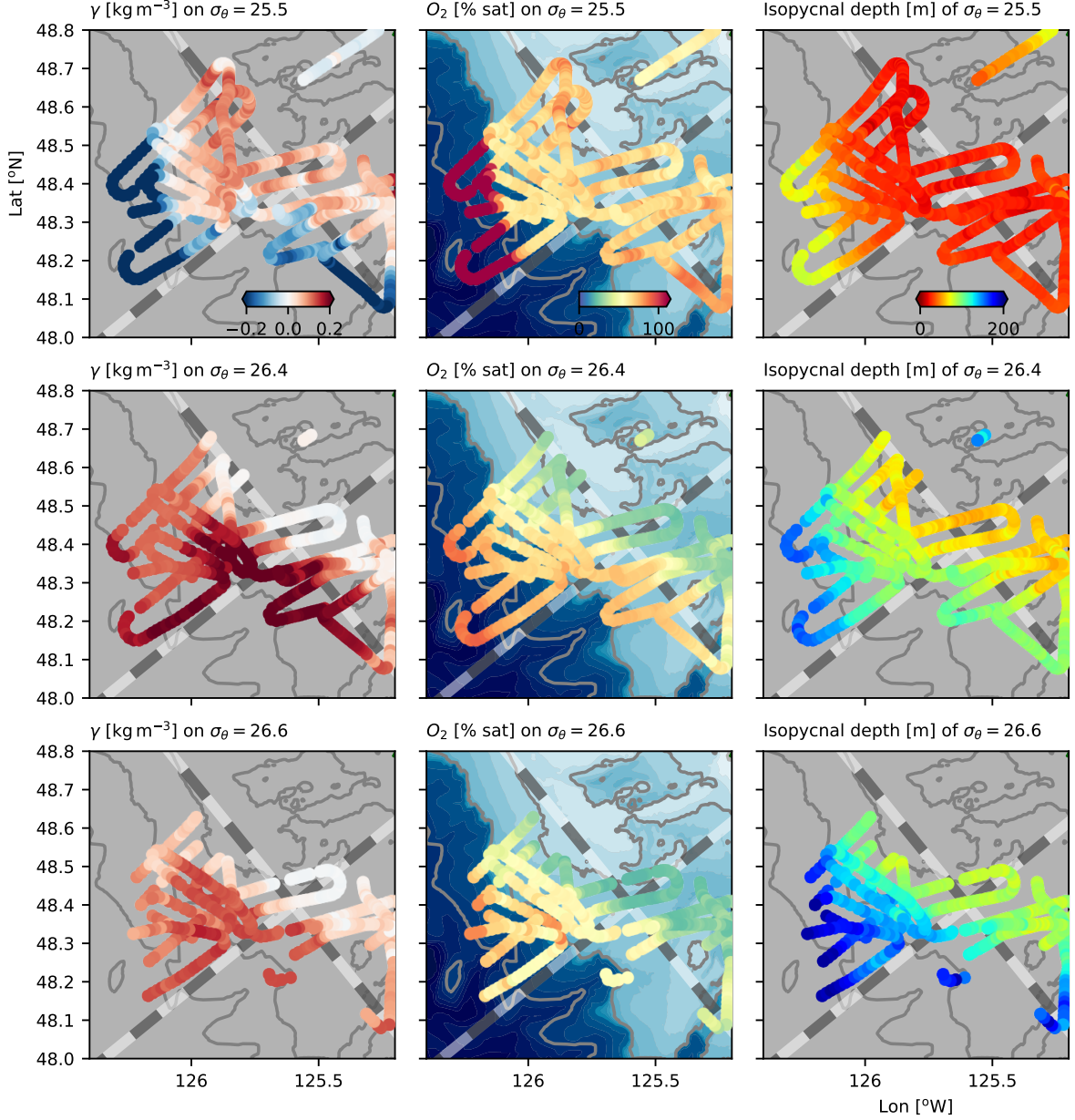


Figure 12. Isopycnal slices through showing the vertical structure of the water separating from the shelf, with the first row along 25.5 kg m^{-3} , second along 26.4 kg m^{-3} , and the third at 26.6 kg m^{-3} . First column is the spice anomaly, second is oxygen saturation, and the last column is depth of each isopycnal.

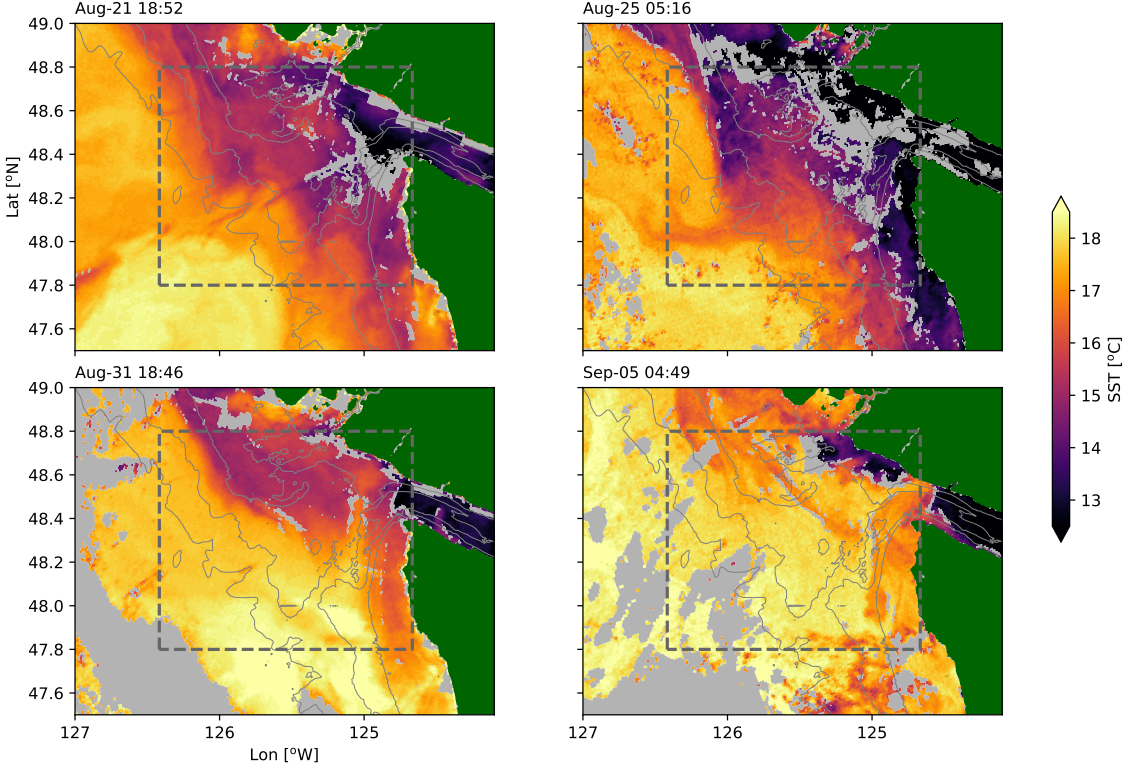


Figure 13. Sea surface temperature snapshots from the observation period. Grey areas are clouds; dashed gray line is the study area. Depths are contoured in thin gray lines at 200, 150 and 100 m. (OSI SAF, 2015)

the feature, though small tendrils of cooler water can be seen separating from La Perouse Bank. By 5 September, the water has significantly warmed, and the offshore anomaly does not appear to have a surface signature.

Satellite-based surface chlorophyll estimates show the same feature (figure 14) demonstrating the advection of high chlorophyll to the west side of the EDDY. They also show a relatively high-chlorophyll tendril to the west, again exiting the study region at approximately 48 degrees N. The feature is relatively long-lived, on the order of one month. Inspection of images before August 5 were too obscured by clouds or did not show this feature. By September 6, we see the feature fading from the satellite image. Note that this feature is centered 0.2 degrees of latitude south of tongue that we observe deeper in the water column, again indicating that there is depth-dependent structure in the feature.

4 Summary and Discussion

The intensive sampling discussed here has demonstrated a few important features of the South Vancouver Island Shelf. The Juan de Fuca Eddy water is readily identified as falling along a mixing line in $\theta - S$ space, compared with offshore water that was warmer and saltier (high-salinity anomaly). There was not strong evidence of the EDDY being supplied by water moving up the Spur Canyon during our observations, but the Spur Canyon was a site of hydraulic cross-canyon flows in which we infer significant mixing. There is a sharp and persistent temperature-salinity compensated front between offshore water and the partially mixed EDDY water. Finally, upstream of the EDDY, water in the equatorward shelf current

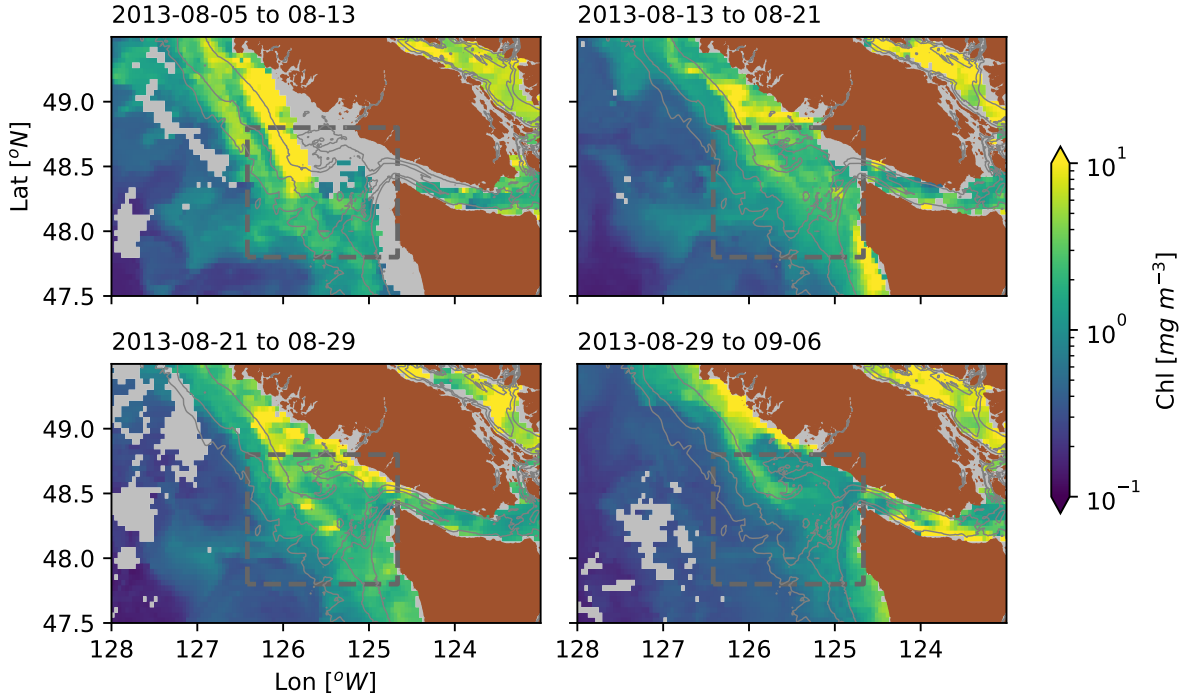


Figure 14. Surface chlorophyll density estimated from ocean color (Hu et al., 2012; NASA Ocean Biology Processing Group, 2017) over 8-day windows in 4-km bins. Gray regions had too many clouds to compute averages.

has intermediate spice anomaly, and is seen to separate from the shelf at the point of an abrupt bend in an underwater bank. The water mass crosses isobaths and is ejected into the interior. This separation event can also be observed from satellite measurements of sea surface temperature and chlorophyll. Thus the water that is offshore of the EDDY appears to have been brought onto the shelf in exchange for the offshore ejection of shelf water via this tongue.

4.1 Age and source of the EDDY water

The source of water and formation mechanism of the Juan de Fuca Eddy has received substantial attention, however, the observations of EDDY waters being found along a tight mixing line in θ - S space has not previously been noted. The deepest water in the EDDY could originate along the θ - S line from approximately 5.5°C to 7.5°C (figure 4a), which in the open ocean spans depths from 420 m to 70 m. Mackas et al. (1987) attempted to determine the origin of the water by including oxygen as a third variable to resolve the ambiguous θ - S relation. However, as figure 4b makes clear, oxygen does not appear to be a conserved property in the EDDY, with concentrations up to 150 $\mu\text{mol kg}^{-1}$ lower in the EDDY than the water found offshore, and in a way that definitely cannot be the result of conservative mixing. As a best guess, if the water in the deepest part of the EDDY came from a vertical mixture of the water at 26.5 kg m^{-3} and an equal distance down in density space of 26.7 kg m^{-3} , then the deepest water in the EDDY may be coming from a depth of 250 m. This is a typical upwelling depth for coastal flows, and may not require extra input up the Spur Canyon as posited by Freeland and Denman (1982).

375 We found little evidence of flow up the Spur Canyon or, if there is, then the mixing in
 376 the canyon is intense enough to remove the θ - S signature of offshore water within 20 km of
 377 the canyon mouth (figure 9). We did find substantial evidence of mixing in the canyon, but
 378 the primary pathway of high-salinity water into the canyon appears to be due to tidal flow
 379 over the banks on the west side (figure 10), rather than flow up the canyon. However, it is
 380 worthy of note that upwelling winds had ceased at the point of these observations (figure 2),
 381 so the offshore surface pressure gradient may be reduced, leading to reduced ageostrophic
 382 upwelling in the canyon. Whether the cessation of winds would also lead to a reduction of
 383 the low sea level height in the center of the EDDY that may drive up-canyon flow is an open
 384 question.

385 There is evidence of aging of the water in the EDDY between late spring and late
 386 summer (figure 3), with a reduction of oxygen in the EDDY over this time span. If we
 387 posited that the reduction was all in the same water, then the oxygen consumption rate
 388 over the time between the late-May and early September cruises would be on the order of
 389 $0.5 \mu\text{mol kg}^{-1}\text{d}^{-1}$. This is on the low side of estimates of apparent oxygen utilization rates
 390 in continental upwelling systems, which are between 1 and $5 \mu\text{mol kg}^{-1}\text{d}^{-1}$ (Dortch et al.,
 391 1994). So it seems possible the EDDY had enough exchange with the surrounding water for
 392 the residence time to have been less than the full time period from late May to September.
 393 Note that during the May cruise, the water in the EDDY is slightly cooler than the mixing
 394 line, and during the September cruise is slightly warmer than the mixing line, so the water
 395 in the EDDY is evolving seasonally, and probably affected by the water temperature in the
 396 Vancouver Island Coastal Current and the amount of water getting through the onshore
 397 front.

398 The water is mixed enough in the EDDY that it falls along a mixing line, though it
 399 remains vertically stratified. The amount of homogenization is such that either the mixing is
 400 very strong, or the water is retained in the EDDY for a long time. The amount of turbulence
 401 required to homogenize 100 m of water over 90 days is $\kappa \approx 10^{-3} \text{ m}^2\text{s}^{-1}$. Given that the
 402 diffusivity implied in the cross-channel surveys was on the order of $\kappa_\rho = 10 \text{ m}^2\text{s}^{-1}$, this
 403 number is not outrageous if we think that such high dissipation is found in 10^{-4} of the
 404 water column. We can more carefully quantify this by considering a synthetic profile or
 405 temperature and salinity based on an offshore profile, extrapolated from the bottom of the
 406 200-m cast to 250 m, assuming that the temperature and salinity at 250 m are $6.2 [\text{°C}]$ and
 407 34 psu respectively (figure 15). Water at the offshore station was warmer than onshore, so
 408 the profile was also linearly interpolated to a surface value of (12 °C , 31.6 psu). The profile
 409 was then linearly compressed into a depth range of 150 m representative of the shelf depth in
 410 the dense pool, and subjected to mixing with a constant diffusivity of $\kappa = 10^{-3} \text{ m}^2\text{s}^{-1}$, with
 411 the surface and bottom values pinned under the assumption that the near-bottom source
 412 and surface waters are replenished from a large reservoir. Similar to the naive scaling, the
 413 T-S relationship does not approach a straight line until after approximately 60-100 days, or
 414 until the mixing affects a vertical length scale of $\lambda = (\tau\kappa)^{1/2}$ that is greater than $\approx 70 \text{ m}$.

415 The sharpness of the front with the EDDY and the offshore water is intriguing. It was
 416 persistent for the duration of our detailed survey (figure 8), and, so far as we can tell with
 417 the limited resolution of the hydrographic surveys, was present during the bracketing La
 418 Perouse cruises. There is not any substantial bathymetry blocking the onshore incursion of
 419 water at this location, so there must be a dynamic barrier.

420 Numerical simulations of this region reported by (Sahu et al., 2022) using a NEMO
 421 36th-degree regional model contained relatively rapid exchange between the deep EDDY
 422 water and the rest of the coastal ocean. The region where the EDDY resides has velocities
 423 equal or greater than other parts of the shelf, and water has an approximate residence time
 424 of less than 20 days. The EDDY water in the model does develop a distinct θ - S signature,
 425 but not along a sharp mixing line as observed. It also has a front with the offshore water,
 426 but the front is substantially wider than that observed here.

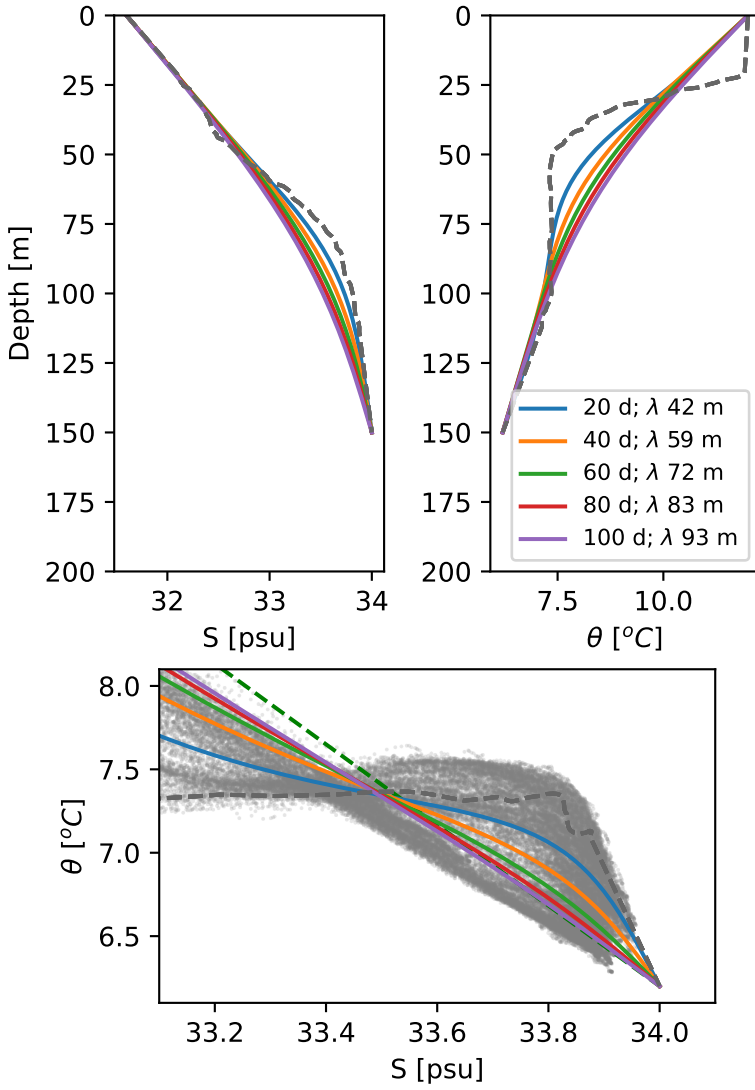


Figure 15. Mixing model assuming constant eddy diffusivity of $\kappa = 10^{-3} \text{ m}^2 \text{s}^{-1}$ acting on an offshore temperature and salinity profiles compressed from 250 thick to 150 m thick (grey dashed lines). Profiles are pinned to the deep $\theta - S$ value at (34 psu, 6.2 °C), and a shallow one at (31.6 psu, 12 °C). The green dashed line is the mixing line defined in the text.

427 Overall, it would be an improvement to our understanding of the EDDY if we could
 428 sample the shelf more persistently. The EDDY was already well-formed by the May La
 429 Perouse cruise, and seems to evolve slowly during that time. Capturing its formation,
 430 presumably earlier in the spring, as well as its evolution through the year, would be valuable
 431 in understanding retention and exchange on this productive part of the shelf.

432 4.2 Offshore exchange of shelf water

433 The displacement of shelf water from La Perouse Bank is a dramatic departure from
 434 geostrophically balanced isobath-following flow. Eddies have been known to separate from
 435 irregular coastal topography, both at the surface (Barth et al., 2000) and deeper in the
 436 water column (Pelland et al., 2013). It has been recognized that instabilities lead to exchange
 437 between the open ocean and the shelf at this location (Ikeda & Emery, 1984, 1984). However,
 438 observations of the wholesale replacement of shelf water by a new water mass from offshore
 439 are rare. In the observations presented here, it is clear that water from as deep as 150 m is
 440 separating from the shelf and moving offshore (figure 8, figure 12).

441 Satellite imagery shows that there is often exchange between coastal and deep waters
 442 along the Vancouver Island shelf (figure 16). Most years there are three of four large filaments
 443 from the shelf into the open ocean, many of them over 100 km long. This length scale is
 444 longer than the 60 km inferred for this region by Ikeda et al. (1984) using a four-layer
 445 instability analysis. It is possible that there is spatial locking of these features, with a
 446 persistent separation at the north tip of Vancouver Island, and a strong tendency for one
 447 at 49.5 N. There is also evidence of separation events in most of the years, with 2011
 448 being the only clear exception. General baroclinic instability of the upwelling front is a
 449 possible mechanism to drive offshore exchange (Ikeda et al., 1984; Durski & Allen, 2005),
 450 but this tends to be shallow, with smaller-scale instabilities that will not extend as far into
 451 the interior ocean as observed here. Rather it seems likely that the topographic change
 452 engendered by the sudden turn to the east of La Perouse bank catalyses a larger scale
 453 instability at this location. Durski and Allen (2005), when modelling the Oregon shelf,
 454 found that including realistic shelf bathymetry catalyzed intermittent large-scale instabilities
 455 similar to the feature here, a finding that is deemed likely to apply at other coastal locations
 456 (Batteen, 1997).

457 Large-scale mixing between the shelf and open ocean has been evident since the satellite
 458 era. Here we demonstrate that in the Vancouver Island shelf the flow is originating on the
 459 shelf and separating from the bathymetry and being injected into the interior. A similar
 460 observation was made by Barth et al. (2000) downstream of Cape Blanco, Oregon, where
 461 the coastal current was observed to detach from the shelf in the lee of the cape and flow into
 462 the interior. They hypothesized that as the current moved offshore, it deepened, stretching
 463 isopycnals and creating cyclonic relative vorticity that would tend to push the current back
 464 onshelf, but then it was caught in the undercurrent and stalled, being pushed offshore. It is
 465 also possible that coastally trapped waves in the region experience a hydraulic control, and
 466 these separation events are part of the response (Dale & Barth, 2001).

467 Regardless of the dynamics of the separation events, the offshore transport can be
 468 substantial. If we assume the coastal current is approximately 0.1 m s^{-1} over 100 m in the
 469 vertical and 20 km in the horizontal, it represents 0.2 Sv of nutrient- and chlorophyll-rich
 470 shelf water transported offshore. Our observations are a finer detailed representation of the
 471 kind of cross-shore transports inferred by Mackas and Yelland (1999) from hydrographic
 472 surveys, and definitively show that this water can originate from the shelf from relatively
 473 deep depths and be transported offshore. We do not have velocity measurements for the
 474 water that replaces it, but assuming that water also flows along-shelf, these separation
 475 events are associated with a large replacement of shelf water with offshore water at this
 476 location. This emphasizes the importance of three dimensional observations and modeling
 477 of cross-shelf dynamics when thinking about physical and biological processes on the shelf.

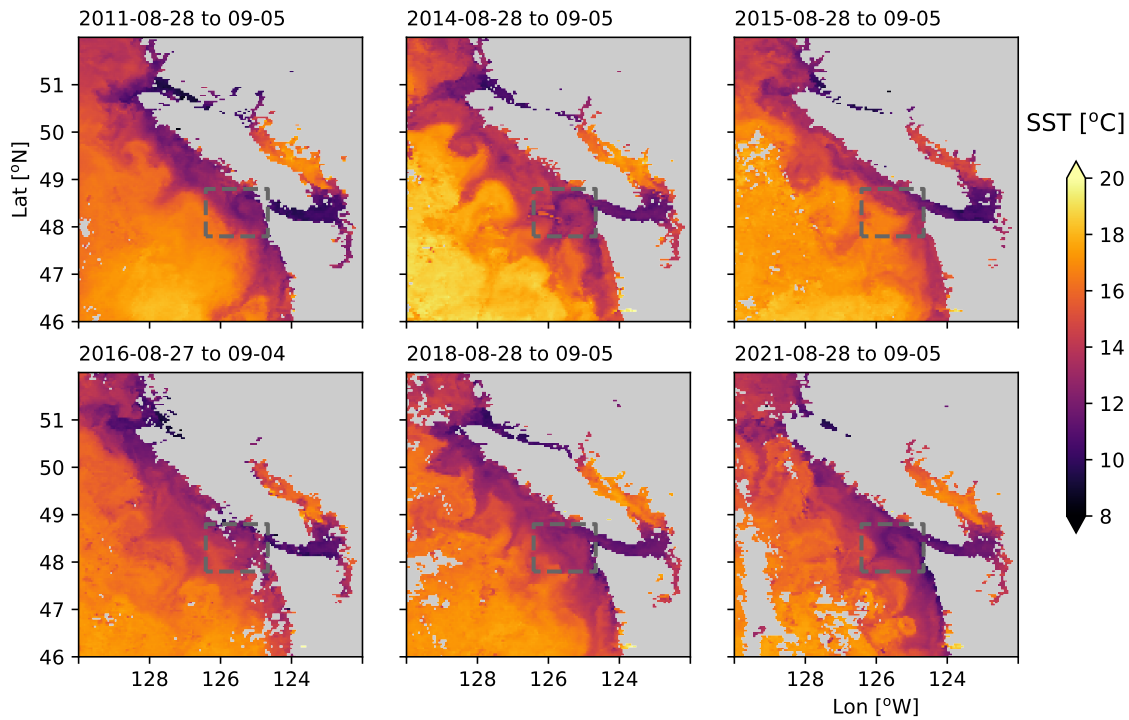


Figure 16. Available late-August sea-surface temperature from 8-day composites, 2011 to 2021 (NASA Ocean Biology Processing Group, 2019); missing years had too much cloud cover or no satellite coverage.

478 Open Research

479 Derived data files (1-m vertical binned CTD files) and analysis scripts are available at
 480 <https://ocean-physics.seos.uvic.ca/~jklymak/PW13DataAnalysis/>. Raw CTD data
 481 is available on request. Data was processed using a scientific python toolchain as listed at
 482 <https://ocean-physics.seos.uvic.ca/~jklymak/PW13DataAnalysis/environment.yml>;
 483 major components include xarray (Hoyer & Hamman, 2017), numpy (Harris et al., 2020),
 484 and Matplotlib (Caswell et al., 2022), but those all leverage many smaller but vital projects.

485 Acknowledgments

486
 487 Thank you to the officers and crew of the R/V Falkor and the Schmidt Foundation
 488 for funding the seagoing component of the cruise. Thank you to Richard Dewey, Benjamin
 489 Schieffe, and Rowan Fox for efforts during the cruise. Klymak was supported by NSERC
 490 Discovery grant RGPIN-2017-04050 and a Canadian Foundation for Innovation Leading
 491 Edge Fund grant 36109, Allen was supported by NSERC Discovery grant RGPIN-105694-
 492 11, and Waterman was supported by NSERC Discovery grant RGPIN-2020-05799.

493 References

- 494 Barth, J. A., Pierce, S. D., & Smith, R. L. (2000). A separating coastal upwelling jet at
 495 Cape Blanco, Oregon and its connection to the California Current system. *Deep Sea*
 496 *Res. II*, 47(5–6), 783 - 810. doi: [http://dx.doi.org/10.1016/S0967-0645\(99\)00127-7](http://dx.doi.org/10.1016/S0967-0645(99)00127-7)
- 497 Batteen, M. L. (1997). Wind-forced modeling studies of currents, meanders, and eddies in
 498 the California Current system. *J. Geophys. Res.*, 102(C1), 985–1010. doi: [10.1029/96jc02803](https://doi.org/10.1029/96jc02803)
- 499 Brink, K. (2016). Cross-shelf exchange. *Annu. Rev. Mar. Sci.*, 8(1), 59–78. doi: [10.1146/annurev-marine-010814-015717](https://doi.org/10.1146/annurev-marine-010814-015717)
- 500 Castelao, R. M., & Barth, J. A. (2007, nov). The role of wind stress curl in jet separation
 501 at a cape. *J. Phys. Oceanogr.*, 37(11), 2652–2671. doi: [10.1175/2007jpo3679.1](https://doi.org/10.1175/2007jpo3679.1)
- 502 Caswell, T. A., Lee, A., Droettboom, M., De Andrade, E. S., Hoffmann, T., Klymak, J.,
 503 ... Kniazev, N. (2022). *matplotlib/matplotlib: Rel: v3.6.0*. Zenodo. Retrieved from
<https://zenodo.org/record/7084615> doi: [10.5281/ZENODO.7084615](https://doi.org/10.5281/ZENODO.7084615)
- 504 Dale, A. C., & Barth, J. A. (2001, jan). The hydraulics of an evolving upwelling jet flowing
 505 around a cape. *Journal of Physical Oceanography*, 31(1), 226–243. doi: [10.1175/1520-0485\(2001\)031<0226:thoaeu>2.0.co;2](https://doi.org/10.1175/1520-0485(2001)031<0226:thoaeu>2.0.co;2)
- 506 D'Asaro, E. A., Shcherbina, A. Y., Klymak, J. M., Molemaker, J., Novelli, G., Guigand,
 507 C. M., ... Özgökmen, T. M. (2018, Jan). Ocean convergence and the dispersion of
 508 flotsam. *Proc. Natl. Acad. Sci. U.S.A.*, 201718453. doi: [10.1073/pnas.1718453115](https://doi.org/10.1073/pnas.1718453115)
- 509 Dewey, R. K., & Crawford, W. R. (1988). Bottom stress estimates from vertical dissipation
 510 rate profiles on the continental shelf. *J. Phys. Oceanogr.*, 18, 1167–1177.
- 511 DFO. (2022). *Marine environmental data section archive, buoy c46206*. Ecosystem and
 512 Oceans Science, Department of Fisheries and Oceans Canada. Retrieved 2022-01-31,
 513 from <https://meds-sdmm.dfo-mpo.gc.ca>
- 514 Dortch, Q., Rabalais, N. N., Turner, R. E., & Rowe, G. T. (1994, dec). Respiration rates
 515 and hypoxia on the Louisiana shelf. *Estuaries*, 17(4), 862. doi: [10.2307/1352754](https://doi.org/10.2307/1352754)
- 516 Durski, S. M., & Allen, J. S. (2005). Finite-amplitude evolution of instabilities associated
 517 with the coastal upwelling front. *J. Phys. Oceanogr.*, 35(9), 1606–1628. doi: [10.1175/jpo2762.1](https://doi.org/10.1175/jpo2762.1)
- 518 Engida, Z., Monahan, A., Ianson, D., & Thomson, R. E. (2016). Remote forcing of sub-
 519 surface currents and temperatures near the northern limit of the California Current
 520 system. *J. Geophys. Res.*, 121(10), 7244–7262. doi: [10.1002/2016jc011880](https://doi.org/10.1002/2016jc011880)
- 521 Foreman, M. G. G., Callendar, W., MacFadyen, A., Hickey, B. M., Thomson, R. E., &
 522 Lorenzo, E. D. (2008). Modeling the generation of the Juan de Fuca Eddy. *J.*

- 528 *Geophys. Res.*, 113(C3). doi: 10.1029/2006jc004082
- 529 Freeland, H., & Denman, K. (1982). A topographically controlled upwelling ceter off
530 southern Vancouver Island. *J. Mar. Res.*, 40(4), 1069–1093.
- 531 Freeland, H., & McIntosh, P. (1989). The vorticity balance on the southern British Columbia
532 continental shelf. *Atmosphere–Ocean*, 27(4), 643–657.
- 533 Harris, C. R., Millman, K. J., van der Walt, S. J., Gommers, R., Virtanen, P., Cournapeau,
534 D., ... Oliphant, T. E. (2020, sep). Array programming with NumPy. *Nature*,
535 585(7825), 357–362. Retrieved from <https://doi.org/10.1038%2Fs41586-020-2649-2>
536 doi: 10.1038/s41586-020-2649-2
- 537 Hickey, B., Thomson, R., Yih, H., & LeBlond, P. (1991). Velocity and temperature fluctu-
538 ations in a buoyancy-driven current off Vancouver Island. *J. Geophys. Res.*, 96(C6),
539 10,507–10,538.
- 540 Hoyer, S., & Hamman, J. (2017, apr). xarray: N-d labeled arrays and datasets in python.
541 *Journal of Open Research Software*, 5(1), 10. Retrieved from <https://doi.org/10.5334%2Fjors.148>
542 doi: 10.5334/jors.148
- 543 Hu, C., Lee, Z., & Franz, B. (2012). Chlorophyll a algorithms for oligotrophic oceans: A
544 novel approach based on three-band reflectance difference. *J. Geophys. Res.*, 117(C1).
545 doi: 10.1029/2011jc007395
- 546 Ikeda, M., & Emery, W. J. (1984). A continental shelf upwelling event off Vancouver
547 Island as revealed by satellite infrared imagery. *J. Mar. Res.*, 42(2), 303–317. doi:
548 10.1357/002224084788502774
- 549 Ikeda, M., Mysak, L. A., & Emery, W. J. (1984). Observation and modeling of satellite-
550 sensed meanders and eddies off Vancouver Island. *J. Phys. Oceanogr.*, 14(1), 3–21.
551 doi: 10.1175/1520-0485(1984)014<0003:oa moss>2.0.co;2
- 552 Klymak, J. M., Crawford, W., Alford, M. H., MacKinnon, J. A., & Pinkel, R. (2015).
553 Along-isopycnal variability of spice in the North Pacific. *J. Geophys. Res.*, 2169-9291.
554 doi: 10.1002/2013JC009421
- 555 Klymak, J. M., Shearman, R. K., Gula, J., Lee, C. M., D’Asaro, E. A., Thomas, L. N., ...
556 others (2016). Submesoscale streamers exchange water on the north wall of the Gulf
557 Stream. *Geophys. Res. Lett.*. doi: 10.1002/2015GL067152
- 558 MacFadyen, A., & Hickey, B. M. (2010). Generation and evolution of a topographically
559 linked, mesoscale eddy under steady and variable wind-forcing. *Cont. Shelf Res.*,
560 30(13), 1387–1402. doi: 10.1016/j.csr.2010.04.001
- 561 Mackas, D. L., Denman, K. L., & Bennett, A. F. (1987). Least squares multiple tracer
562 analysis of water mass composition. *J. Geophys. Res.*, 92(C3), 2907–2918.
- 563 Mackas, D. L., & Yelland, D. R. (1999, nov). Horizontal flux of nutrients and plankton
564 across and along the British Columbia continental margin. *Deep Sea Res. II*, 46(11-
565 12), 2941–2967. doi: 10.1016/s0967-0645(99)00089-2
- 566 NASA Ocean Biology Processing Group. (2017). *MODIS-aqua level 3 mapped chloro-*
567 *phyll data version r2018.0*. NASA Ocean Biology DAAC. Retrieved from <https://oceancolor.gsfc.nasa.gov/data/10.5067/AQUA/MODIS/L3M/CHL/2018> doi: 10
568 .5067/AQUA/MODIS/L3M/CHL/2018
- 569 NASA Ocean Biology Processing Group. (2019). *MODIS-aqua level 3 mapped SST data*
570 *version r2019.0*. NASA Ocean Biology DAAC. Retrieved from https://oceandata.sci.gsfc.nasa.gov/ob/getfile/AQUA_MODIS
- 571 OSI SAF. (2015). *GHRSST level 2p sub-skin sea surface temperature from the Advanced*
572 *Very High Resolution Radiometer (AVHRR) on Metop satellites (currently Metop-A)*
573 *(GDS V2) produced by OSI SAF*. NASA Physical Oceanography DAAC. Retrieved
574 from https://podaac.jpl.nasa.gov/dataset/AVHRR_SST_METOP_A-OSISAF-L2P-v1.0 doi: 10.5067/GHAMA-2PO02
- 575 Pelland, N. A., Eriksen, C. C., & Lee, C. M. (2013). Subthermocline eddies over the
576 washington continental slope as observed by seagliders, 2003-09. *J. Phys. Oceanogr.*
577 doi: 10.1175/JPO-D-12-086.1
- 578 Relvas, P., & Barton, E. D. (2005). A separated jet and coastal counterflow during upwelling
579 relaxation off Cape São Vicente (Iberian Peninsula). *Cont. Shelf Res.*, 25(1), 29–49.
580

- 583 doi: 10.1016/j.csr.2004.09.006
584 Sahu, S., Allen, S. E., Saldías, G. S., Klymak, J. M., & Zhai, L. (2022, mar). Spatial and
585 temporal origins of the La Perouse low oxygen pool: A combined lagrangian statistical
586 approach. *J. Geophys. Res.*, 127(3). doi: 10.1029/2021jc018135
587 Thomson, R. E., & Gower, J. F. R. (1998, feb). A basin-scale oceanic instability event in
588 the gulf of alaska. *J. Geophys. Res.*, 103(C2), 3033–3040. doi: 10.1029/97jc03220
589 Thomson, R. E., Hickey, B. M., & LeBlond, P. H. (1989). The Vancouver Island Coastal
590 Current: Fisheries barrier and conduit. In R. J. Beamish & G. A. McFarlane (Eds.),
591 *Effects of ocean variability on recruitment and an evaluation of parameters used in*
592 *stock assessment models*. Fisheries and Oceans Canada.
593 Thomson, R. E., & Krassovski, M. V. (2015, dec). Remote alongshore winds drive variability
594 of the California Undercurrent off the British Columbia–Washington coast. *J. Geophys.*
595 *Res.*, 120(12), 8151–8176. doi: 10.1002/2015jc011306
596 Weaver, A. J., & Hsieh, W. W. (1987). The influence of buoyancy flux from estuaries
597 on continental shelf circulation. *J. Phys. Oceanogr.*, 17, 2127–2140. doi: 10.1175/
598 1520-0485(1987)017<2127:TIOBFF>2.0.CO;2